DOI 10.5162/Ultrasonic2025/A15-c3

A Full-Focusing Ultrasound Phased Array Imaging Method Based on MDMAS

Yiming Wang[1], Jichao Xu[1], Qian Lubin[1], GuoPeng Fan[1], Weiwei Qi[1], Haiyan Zhang[2], Hui Zhang[1], and Wenfa Zhu[1]
[1]Shanghai University of Engineering Science, Shanghai and China
[2]Shanghai University, Shanghai and China
jcxu@sues.edu.cn

Abstract: To address the limited contrast and poor noise suppression of conventional Delay Multiply and Sum (DMAS) beamforming, this paper proposes a correlation-guided nonlinear beamforming method. Multiplication is applied only to highly correlated signal pairs to suppress incoherent noise, and a Modified Coherence Factor is introduced to enhance image contrast. Experiments on rail specimens with artificial defects show improved flaw visibility and image clarity over DMAS, demonstrating the proposed method's potential for reliable phased array ultrasonic imaging.

Keywords: Phased array ultrasonic, Beamforming, Correlation, MDMAS, Contrast.

Introduction

Phased array ultrasonic imaging has been widely applied in industrial non-destructive testing and medical diagnostics [1-3]. However, during wave propagation in a medium, scattering and absorption-induced attenuation often lead to severe energy loss [4–5], causing the imaging results to be overwhelmed by noise and resulting in degraded image quality and ineffective defect identification [6–7]. Consequently, enhancing overall imaging performance, which depends on multiple factors such as noise suppression, contrast and signal coherence, has become both a pressing challenge and a central topic in recent ultrasonic imaging research.

The Full Matrix Capture (FMC)-based Total Focusing Method is a typical beamforming algorithm [8]. Based on the Delay and Sum (DAS) strategy, this method reconstructs ultrasonic images, enhancing imaging quality. However, DAS cannot effectively suppress interference signals, the SNR of Total-Focusing images is still insufficient [9-11]. In recent years, the Delay Multiply and Sum (DMAS) algorithm, a type of nonlinear beamforming method, has been introduced for use in medical imaging applications [12]. The distinction between coherent signals (e.g., defect echoes) and incoherent noise is emphasized in DMAS through the multiplication and accumulation of delayed signals., improving SNR by leveraging the spatial coherence of ultrasound signals. While DMAS has shown notable advantages, its performance can still be constrained by incoherent noise and reduced contrast in challenging imaging conditions.

To more effectively improve the SNR and image contrast, a phased array ultrasonic imaging method based on the nonlinear DMAS beamforming algorithm is investigated in this study. The proposed method introduces a threshold value to identify highly correlated signals, applying multiplication only to these signal pairs to adaptively suppress incoherent noise based on their Correlation Coefficient (CC). Since the reduction in multiplied pairs may degrade image contrast, a Modified Coherence Factor (MCF) further applied selectively to the highly correlated signals to enhance contrast. These enhancements collectively define the MDMAS beamforming method.

Methodology

DAS

The signal delayed at the *i*-th element in a phased array consisting of N uniformly spaced elements is represented as $s_i(t-\tau_i(x,z))$ .The DAS beamforming method reconstructs the image without any complex processing of the scattered signals. By summing the delayed signals, this method constructs the final image:

$$y_{DAS}(x,z)=\sum_{i=1}^{N} s_i(t-\tau_i(x,z)) \tag{1}$$

Characterized by simplicity in computation and effective suppression of clutter and noise, DAS is a commonly used data-independent beamforming technique. However, the weights in DAS are independent of the input signal. As a result, images reconstructed using DAS often suffer from high sidelobe levels and low contrast [14-15].

DMAS and Coherence Factor (CF)

$$\begin{aligned}\hat{s}_{ij}(x,z)&=s_i(t-\tau_i(x,z))s_j(t-\tau_j(x,z))\\ y_{DMAS}(x,z)&=\sum_{i=1}^{N-1}\sum_{j=i+1}^{N}\hat{s}_{ij}(x,z)\end{aligned} \tag{2}$$

The DMAS beamforming method achieves better sidelobe suppression and improved contrast by multiplying delayed signals. Eq. (2) illustrates the DMAS algorithm, where and are the delayed signals received by the i-th and j-th elements, respectively. Each pair of delayed signals is multiplied.

$$CF(x,z)=\frac{\left|\sum_{i=1}^{N} s_i(t-\tau_i(x,z))\right|^2}{N\sum_{i=1}^{N}\left|s_i(t-\tau_i(x,z))\right|^2} \tag{3}$$

A band-pass filter is used at the final stage to preserve the second harmonic signal [16], forming the DMAS beamformer. The CF is an adaptive weighting factor that reflects the ratio between coherent and incoherent signal energy. The traditional CF is defined as Eq. (3).
CF can be used to weight the output of DMAS beamforming, as shown in Eq. (4):

$$y_{DMAS}'(x,z) = CF(x,z) \times y_{DMAS}(x,z) \tag{4}$$

MDMAS and MCF
The CC is computed for every possible pair of received signals, denoted as ρ . In other words, $\rho(s_i, s_j)$ represents the CC between the ultrasound signals received by the *i*-th and *j*-th elements:

$$\rho(s_i, s_j) = \frac{COV(s_i, s_j)}{\sigma(s_i)\sigma(s_j)} \tag{5}$$

In this context, the delayed signals received by the *i*-th and *j*-th elements are denoted as s_i and s_j , respectively. $COV(s_i, s_j)$ serves as a measure of the covariance between the two signals, and $\sigma(s_i)$, $\sigma(s_j)$ are their standard deviations.
In Eq. (6), ultrasound signals with CC values lower than a predefined threshold value are excluded. The MDMAS beamforming method which doesn't have MCF can be expressed as:

$$y_{MDMAS}'(x,z) = \sum_{i=1}^{N-1} \sum_{j=i+1}^{N} \hat{s}_{ij}(x,z) \quad subject\ to \quad \rho(s_i, s_j) \geq threshold\ value \tag{6}$$

By applying the MCF to the MDMAS beamforming method (without MCF), the image contrast is enhanced and sidelobes are suppressed. The MCF can be expressed as:

$$MCF(x,z) = \frac{\left|\sum_{j \in E} s_j(t - \tau_j(x,z))\right|^2}{M \sum_{j \in E} \left|s_j(t - \tau_j(x,z))\right|^2} \tag{7}$$

Let *M* denote the length of *E*, representing the number of ultrasound signals satisfying the threshold value. The MCF is then incorporated into the beamforming scheme based on the proposed DMAS. The resulting beamforming formulation is expressed as:

$$y_{MDMAS}(x,z) = y_{MDMAS}'(x,z) \times MCF(x,z) \tag{8}$$

The structural overviews of DAS, DMAS, and MDMAS beamforming methods are illustrated in Fig. 1.

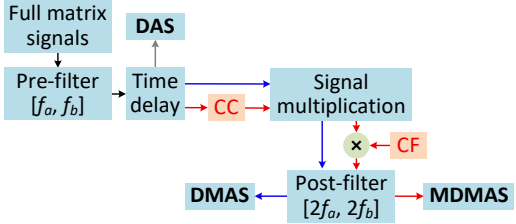

Fig. 1 Flowcharts of the DAS, DMAS, and MDMAS beamforming methods and their combinations with the MCF.

Contrast (CR) [17] and Signal-to-Noise Ratio (SNR) [18] served as quantitative metrics for evaluating the performance of the proposed method.

$$CR = 20\log_{10}\left(\frac{S_i}{S_o}\right) \tag{9}$$

$$SNR = 20\log_{10}\left(\frac{S_i}{\sigma_o}\right) \tag{10}$$

where S_i denotes the average signal amplitude in the target defect region at the same imaging depth, S_o and σ_o represent the average signal amplitude and standard deviation of the background region at the same imaging depth, respectively.

Experimental Setup
The experimental data in this study were acquired using a 32-channel ultrasonic phased array inspection system manufactured by M2M (France). Parameter configuration and signal visualization were carried out using the Multi2000 software, as shown in Fig. 2. The test specimen was a rail sample containing artificial defects with a diameter of 5 mm. A 16-element phased array probe manufactured by Shantou Ultrasound Co., Ltd. (China) was used in the experiment. With each element measuring 1.8 mm in width and spaced 0.2 mm apart, the array yields a total aperture of 31.8 mm. The center frequency of probe is about 1 MHz.

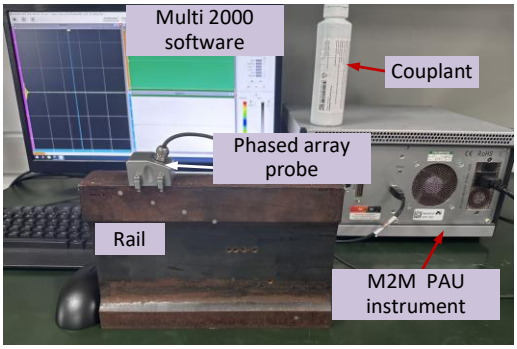

Fig. 2 Experimental system setup.

As shown in Fig. 3, the tested rail specimen contains artificial defects, all of which have a diameter of 5 mm. Region 1 includes a single defect, whereas Region 2 contains two defects with a vertical spacing of 10 mm. These two regions correspond to the imaging scenarios for single and double defects, respectively.

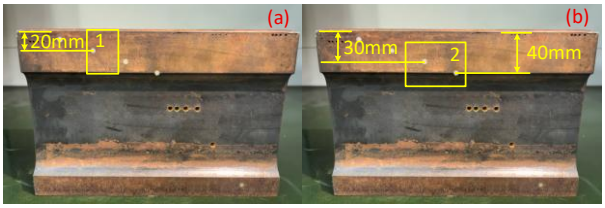

Fig. 3 Tested rail samples: (a) single artificial defect; double artificial defects.

Imaging Results

Imaging Results for One Defect
DAS, DMAS, and MDMAS beamforming methods were applied to the FMC data collected from Region 1 for ultrasonic imaging. The imaging results are shown in Fig.

4. The DAS result contains significant artifacts, due to conventional Total Focusing imaging relies solely on amplitude information, which is susceptible to noise. The DMAS algorithm improves image quality by enhancing the energy of defect signals through multiplication, thereby improving contrast and clarity. MDMAS further improves image quality by adaptively enhancing signal coherence.

The CR and SNR for the three methods were calculated, as shown in Tab.1. In terms of CR, the trend is $CR_{DAS}<CR_{DMAS}<CR_{MDMAS}$; MDMAS improves contrast by 78.72% compared to DAS, and DMAS improves it by 56.79%. In terms of SNR, the trend is $SNR_{DAS}<SNR_{DMAS}<SNR_{MDMAS}$; MDMAS increases SNR by 34.36% over DAS, while DMAS improves it by 22.63%.

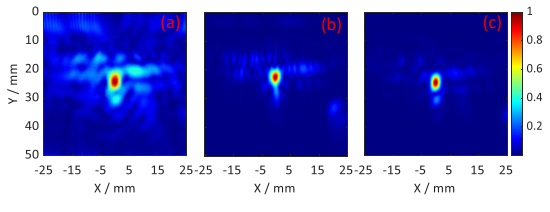

Fig. 4 Imaging results for one defect: (a) DAS; (b) DMAS; (c) MDMAS.

Tab.1 The CR and SNR of one defect's imaging results.

Method	CR (dB)	SNR (dB)
DAS	18.84	19.53
DMAS	29.54	23.95
MDMAS	33.67	26.24

Imaging Results for Two Defects

Ultrasound signals collected from Region 2 were used to image by DAS, DMAS, and MDMAS methods. The results are shown in Fig. 5. It is evident that image quality improves progressively with each algorithm enhancement.

The CR and SNR values of three methods are listed in Tab. 2. In terms of CR, the trend remains $CR_{DAS}<CR_{DMAS}<CR_{MDMAS}$. Both DMAS and MDMAS significantly improve image contrast, such as DMAS improving CR by 39.80% over DAS, and MDMAS improving CR by 9.04% over DMAS. Regarding SNR, the relationship holds $SNR_{DAS}<SNR_{DMAS}<SNR_{MDMAS}$. Specifically, DMAS increases SNR by 14.03% relative to DAS, while MDMAS further enhances SNR by 9.12% compared to DMAS.

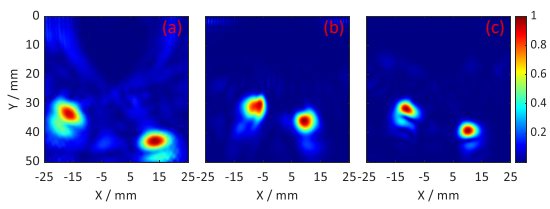

Fig. 5 Imaging results for two defects: (a) DAS; (b) DMAS; (c) MDMAS.

Tab.2 The CR and SNR of two defect's imaging results.

Method	CR (dB)	SNR (dB)
DAS	19.55	17.11
DMAS	27.33	19.51
MDMAS	29.80	21.29

Conclusion

In this study, a modified beamforming method (MDMAS) is proposed to address the problems that insufficient contrast and poor noise suppression of the conventional DMAS algorithm. The proposed method adaptively applies multiplication only to signal pairs with high correlation, which effectively suppresses incoherent components while preserving flaw-related signals. In addition, a MCF is introduced and selectively applied to these pairs of coherent signals, aiming to further improve image contrast. Experimental validation was conducted on rail specimens. Quantitative results showed that, compared to DMAS, the MDMAS method improved the CR by at least 9.04% and the SNR by at least 9.12%. These enhancements result in clearer flaw boundaries and more reliable defect characterization, demonstrating the method's practical potential in rail defect detection and maintenance.

Acknowledgments

This research was funded by the National Natural Science Foundation of China (Grant Nos. 12474457, 12174245, 12374443, 12304514, and 12104290), the National Key Research and Development Program of China (2022YFF0605600), the National Natural Science Foundation of China (Grant No. 12304514) and the Shanghai Municipal Natural Science Foundation (Grant No.24ZR1427300).

References

[1] Mohammadkhani R, Zanotti Fragonara L, Padiyar M J, et al. Improving depth resolution of ultrasonic phased array imaging to inspect aerospace composite structures[J]. *Sensors*, 2020, 20(2): 559.

[2] Fadnes S, Wigen M S, Nyrnes S A, et al. In vivo intracardiac vector flow imaging using phased array transducers for pediatric cardiology[J]. *IEEE transactions on ultrasonics, ferroelectrics, and frequency control*, 2017, 64(9): 1318-1326.

[3] Lin L, Cao H, Luo Z. Total focusing method imaging of multidirectional CFRP laminate with model-based time delay correction[J]. *Ndt & E International*, 2018, 97: 51-58.

[4] Van Pamel A, Brett C R, Lowe M J S. A methodology for evaluating detection performance of ultrasonic array imaging algorithms for coarse-grained materials[J]. *IEEE transactions on ultrasonics, ferroelectrics, and frequency control*, 2014, 61(12): 2042-2053.

[5] Ono K. A comprehensive report on ultrasonic attenuation of engineering materials, including metals, ceramics, polymers, fiber-reinforced composites, wood, and rocks[J]. *Applied Sciences*, 2020, 10(7): 2230.

[6] Villaverde E L, Robert S, Prada C. Ultrasonic imaging in

highly attenuating materials with Hadamard codes and the decomposition of the time reversal operator[J]. *IEEE Transactions on Ultrasonics, Ferroelectrics, and Frequency Control*, 2017, 64(9): 1336-1344.

[7] Jiao J, Ma T, Hou S, et al. A pulse compression technique for improving the temporal resolution of ultrasonic testing[J]. *Journal of Testing and Evaluation*, 2018, 46(3): 1238-1249.

[8] Holmes C, Drinkwater B W, Wilcox P D. Post-processing of the full matrix of ultrasonic transmit–receive array data for non-destructive evaluation[J]. *NDT & e International*, 2005, 38(8): 701-711.

[9] Lines D, Mohseni E, Javadi Y, et al. Using coded excitation to maintain signal to noise for FMC+ TFM on attenuating materials[C]//2019 *IEEE International Ultrasonics Symposium (IUS)*. IEEE, 2019: 635-638.

[10] Da T, Jichao X, Yanxun X, et al. Ultrasonic phased array TFM detection in highly attenuating materials based on modified Golay-coded excitation[C]//2018 *IEEE International Ultrasonics Symposium (IUS)*. IEEE, 2018: 1-4.

[11] Shen C C, Hsieh P Y. Ultrasound baseband delay-multiply-and-sum (BB-DMAS) nonlinear beamforming[J]. *Ultrasonics*, 2019, 96: 165-174.

[12] Lim H B, Nhung N T T, Li E P, et al. Confocal microwave imaging for breast cancer detection: Delay-multiply-and-sum image reconstruction algorithm[J]. *IEEE Transactions on Biomedical Engineering*, 2008, 55(6): 1697-1704.

[13] Deylami A M, Asl B M. Low complex subspace minimum variance beamformer for medical ultrasound imaging[J]. *Ultrasonics*, 2016, 66: 43-53.

[14] Zhu W, Wei Z, Fan G, et al. Ultrasonic guided wave array imaging detection of rail defects based on the symbolic coherent factor total focusing method[J]. *Nondestructive Testing and Evaluation*, 2025: 1-22.

[15] Xing Y, Zhu W, Xu J, et al. Ultrasonic imaging of near-surface blind defects based on WSAttnGAN network[J]. *Measurement*, 2025, 245: 116577.

[16] Matrone G, Savoia A S, Caliano G, et al. The delay multiply and sum beamforming algorithm in ultrasound B-mode medical imaging[J]. *IEEE transactions on medical imaging*, 2014, 34(4): 940-949.

[17] Zheng C, Wang H, Xu X, et al. An adaptive imaging method for ultrasound coherent plane-wave compounding based on the subarray zero-cross factor[J]. *Ultrasonics*, 2020, 100: 105978.

[18] Holmes C, Drinkwater B W, Wilcox P D. Post-processing of the full matrix of ultrasonic transmit–receive array data for non-destructive evaluation[J]. *NDT & e International*, 2005, 38(8): 701-711.